Title

β7 Integrin Inhibition Can Increase Intestinal Inflammation by Impairing Homing of CD25 ^{hi}FoxP3^{+} Regulatory T Cells.

Journal

Cellular and molecular gastroenterology and hepatology, 9(3)

ISSN

2352-345X

Authors

Sun, Hao
Kuk, Wun
Rivera-Nieves, Jesús
et al.

Publication Date

2020

DOI

10.1016/j.jcmgh.2019.10.012

Peer reviewed

cmgh
CELLULAR AND MOLECULAR GASTROENTEROLOGY AND HEPATOLOGY

ORIGINAL RESEARCH

β7 Integrin Inhibition Can Increase Intestinal Inflammation by Impairing Homing of CD25^{hi}FoxP3^{+} Regulatory T Cells

Hao Sun,[1] Wun Kuk,[1] Jesús Rivera-Nieves,[2] Miguel Alejandro Lopez-Ramirez,[1] Lars Eckmann,[3] and Mark H. Ginsberg[1]

[2]Inflammatory Bowel Disease Center, [3]Division of Gastroenterology, [1]Department of Medicine, University of California San Diego, La Jolla, California

SUMMARY

This work proposes that the combination of defective homing and reduced intrinsic regulatory T cell function synergize to reduce regulatory T-cell function sufficiently in the gut to counteract the protective effect of β7 deficiency on homing of conventional T cells, thus exacerbating intestinal inflammation.

BACKGROUND & AIMS: Integrin α4β7 mediates lymphocyte trafficking to the gut and gut-associated lymphoid tissues, a process critical for recruitment of effector lymphocytes from the circulation to the gut mucosa in inflammatory bowel disease (IBD) and murine models of intestinal inflammation. Antibody blockade of β7 integrins generally is efficacious in IBD; however, some patients fail to respond, and a few patients can experience exacerbations. This study examined the effects of loss of β7 integrin function in murine models of IBD.

METHODS: In a mouse IBD model caused by lack of interleukin 10, a cytokine important in CD25^{hi}FoxP3^{+} regulatory T cell (Treg) function, genetic deletion of β7 integrin or antibody blockade of α4β7–mucosal addressin cell adhesion molecule-1 interaction paradoxically exacerbated colitis.

RESULTS: Loss of β7 impaired the capacity of Tregs homing to the gut and therefore suppress intestinal inflammation in an adoptive T-cell transfer model; however, the intrinsic suppressive function of β7-deficient Tregs remained intact, indicating that the β7 deficiency selectively impacts gut homing. Deletion of β7 integrin did not worsen colitis in an acute dextran sodium sulfate model in which Treg number and function were normal.

CONCLUSIONS: In Integrin subunit beta (*Itgb*)$7^{-/-}$*Il10*$^{-/-}$ mice, loss of β7-dependent Treg homing to gut-associated lymphoid tissues combined with loss of intrinsic Treg function exacerbated intestinal inflammation. These results suggest that IBD patients with reduced CD25^{hi}FoxP3^{+} Treg numbers or function or lack of interleukin 10 could be at risk for failure of α4β7 blocking therapy. *(Cell Mol Gastroenterol Hepatol 2020;9:369–385; https://doi.org/10.1016/j.jcmgh.2019.10.012)*

Keywords: Integrin β7 Blockade; Inflammatory Bowel Disease; Regulatory T Cells; Gut-Associated Lymphoid Tissue.

Homeostasis in the gut relies on a fine-tuned interplay of protective immunity against pathogens while maintaining tolerance to the commensal microbiota that comprises much of the intestinal microenvironment. Disruption of homeostasis can lead to intestinal disorders such as inflammatory bowel disease (IBD).[1–4] A key feature of the inflammatory response in IBD is the rapid recruitment of leukocytes from the blood stream to the intestine via cell adhesion and transmigration through blood vessel walls,[5–7] leading to massive infiltration of mononuclear phagocytes, neutrophils, and inflammatory T cells into the intestinal lamina propria.[8–10]

Leukocyte homing to the gut is regulated by a network of adhesion molecules and their ligands to ensure the proper location of immune cells for interaction with the local microenvironment.[11] This process is controlled largely by chemokines, which initiate a multistep adhesion cascade involving tethering, rolling, and cell arrest[12,13] through modulation of integrin binding to endothelial and mucosal ligands (eg, αLβ2/intercellular adhesion molecule-1[ICAM-1], α4β1/vascular cell adhesion molecule-1[VCAM-1], and α4β7/mucosal addressin cell adhesion molecule-1 [MAdCAM-1]).

Blockade of mucosal T-cell homing is a therapeutic approach for IBD.[14] Integrin α4β7, which is expressed on the surface of gut-tropic effector lymphocytes, is an important cell adhesion molecule that mediates lymphocyte trafficking to gut and gut-associated lymphoid tissue (GALT). Vedolizumab, which specifically blocks integrin α4β7, is used for attenuating mucosal inflammation in patients with Crohn's disease (CD) and ulcerative colitis (UC).[15,16] Despite the general effectiveness of vedolizumab, a significant number of IBD patients are

Abbreviations used in this paper: **CD, Crohn's disease; CFSE, carboxyfluorescein succinimidyl ester; DSS, dextran sodium sulfate; GALT, gut-associated lymphoid tissue; GFP, green fluorescent protein; IBD, inflammatory bowel disease; ITGB, Integrin subunit beta; IL, interleukin; MAdCAM-1, mucosal addressin cell adhesion molecule-1; MLN, mesenteric lymph node; PCR, polymerase chain reaction; PLN, peripheral lymph node; PP, Peyer's patch; SP, spleen; Tconv, conventional T cells; TGF, transforming growth factor; Th, helper T cell; Treg, regulatory T cell; UC, ulcerative colitis; WT, wild-type.**

Most current article

2352-345X
https://doi.org/10.1016/j.jcmgh.2019.10.012

nonresponders. The treatment was stopped or optimized because of a lack or loss of response in 36%–54% of IBD patients.[17,18] Moreover, high doses of etrolizumab, which blocks $\beta7$ integrins (ie, $\alpha4\beta7$, $\alpha E\beta7$), is associated with a reduced clinical response.[19] Thus, although $\beta7$ blockade generally is beneficial in IBD, the reason that some patients are nonresponders remains unclear.

$CD25^{hi}Foxp3^{+}$ regulatory T cells (Tregs) can limit the development of colitis by reducing the accumulation and activity of effector cells in the inflamed mucosa.[20–24] Tregs can suppress immune responses by a wide variety of mechanisms, including secretion of immunosuppressive cytokines such as interleukin (IL)10.[25] IL10 is a major immunosuppressive product of Tregs to maintain homeostasis at the environmental interface of the intestine.[26] In addition, IL10-deficient mice develop spontaneous IBD.[27,28] Recent work has indicated that $\alpha4\beta7$ is crucial for homing of Tregs to gut and GALT in patients with UC,[29] and $\beta7$ deficiency causes a reduction of murine Tregs in the gut.[30,31] Here, we report that IL10-deficient mice, which are deficient in the Treg function of IL10 secretion, paradoxically developed exacerbated intestinal inflammation when $\beta7$ was genetically inactivated or $\alpha4\beta7$-mediated gut homing was blocked by antibodies. These effects of loss of $\beta7$ function were associated with a loss of Tregs in the lamina propria owing to reduced Treg homing to the gut. By using an adoptive transfer model of intestinal inflammation, we show that $\beta7$-deficient Tregs are impaired in their capacity to populate the lamina propria and to prevent intestinal inflammation even though they show normal intrinsic suppressive functions. Taken together, these data suggest that the combination of reduced Tregs function in IL10 null mice and reduced Treg homing secondary to loss of $\beta7$ function, in combination, reduce Treg activity in the gut sufficiently to counteract the protective effect of blocking $\beta7$ homing of conventional T cells (Tconv). This conclusion implies that the presence of reduced Treg number or function or reduced IL10 expression could predispose to impaired efficacy of $\beta7$ blockade in IBD.

Results

$\beta7$ Deficiency Exacerbates Spontaneous Colitis in $Il10^{-/-}$ Mice

Integrin $\alpha4\beta7$ mediates trafficking of Tconv to gut and GALT and antibody blockade of $\alpha4\beta7$ benefits many patients with either CD or UC.[15,16] To assess the role of $\beta7$ integrin in the development of chronic intestinal inflammation in a mouse model, we used an IL10-deficient mouse strain (*B6.129P2-Il10tm1Cgn/J*) that develops chronic colitis resembling IBD in human beings.[27,28] IL10-deficient mice were crossed with $\beta7$-deficient mice, and the phenotypes of Integrin subunit beta (*Itgb*)$7^{-/-}Il10^{-/-}$ mice were compared with $Itgb7^{+/+}Il10^{-/-}$ mice.

As expected,[27,28] $Itgb7^{+/+}Il10^{-/-}$ mice spontaneously developed diarrhea beginning at the age of 60–70 days under specific pathogen-free conditions in our animal facility. On average, the mice did not lose weight; however, 6 of 22 mice died by 70 days (Figure 1*B*), and 7 of 22 mice developed rectal prolapse. Unexpectedly, $\beta7$ deficiency exacerbated disease in $Il10^{-/-}$ mice as judged by dramatic weight loss accompanied by severe diarrhea and rectal bleeding (Figure 1*A* and *C*). Furthermore, $Itgb7^{-/-}Il10^{-/-}$ mice almost uniformly developed rectal prolapse (Figure 1*D*) and more than two thirds of them died by approximately 70 days (Figure 1*B*). $Itgb7^{-/-}Il10^{-/-}$ mice were more anemic than integrin $\beta7$–replete $Itgb7^{+/+}Il10^{-/-}$ animals (Figure 1*E*). The exacerbated colitis in $Itgb7^{-/-}Il10^{-/-}$ mice was confirmed by significantly increased crypt distortion, mucosal ulceration, and infiltration of immune cells, compared with $Itgb7^{+/+}Il10^{-/-}$ mice (Figure 1*F* and *G*). In addition, colonic expression of proinflammatory cytokines was increased significantly in $Itgb7^{-/-}Il10^{-/-}$ mice compared with $Itgb7^{+/+}Il10^{-/-}$ mice (Figure 2).

To assess the contribution of $\beta7$ integrin further in mediating leukocyte recruitment and subsequent damage to the gut mucosa, we used piroxicam administration as a method to synchronize development of colitis in IL10-deficient mice.[32] We administered piroxicam to IL10-null mice orally for 2 weeks. By 35 days after piroxicam initiation, approximately 80% of $Itgb7^{-/-}Il10^{-/-}$ mice died. In contrast, only approximately 28% of $Itgb7^{+/+}Il10^{-/-}$ mice died (Figure 1*H*). Thus, $\beta7$ deficiency exacerbated both spontaneous and induced IBD in IL10-deficient mice, a surprising result in light of the benefits of blockade of $\alpha4\beta7$ in many IBD patients.

Integrin $\beta7$ Deficiency Results in Decreased Tregs in the Colon

Integrin $\alpha4\beta7$ mediates lymphocyte trafficking to the intestinal mucosa by binding to its ligand, MAdCAM-1. To investigate whether the severe colitis in $Itgb7^{-/-}Il10^{-/-}$ mice was associated with reduced colonic Tregs, we enumerated Tregs and conventional $CD4^{+}$ T cells in the colonic lamina propria. $Itgb7^{-/-}Il10^{-/-}$ mice showed approximately 75% reduced Tregs in the colonic lamina propria compared with $Itgb7^{+/+}Il10^{-/-}$ mice (Figure 3), consistent with observations in other models.[29–31] In contrast, a slight but statistically significant increase ($P = .02$) in the number of colonic lamina propria $CD4^{+}$ T cells in $Itgb7^{+/+}Il10^{-/-}$ mice was observed, resulting in an approximately 80% reduction of Tregs as a percentage of colonic lamina propria $CD4^{+}$ T cells (Figure 3*A* and *B*). The abundance of Tregs and total $CD4^{+}$ T cells in the spleen was not significantly different between $Itgb7^{-/-}Il10^{-/-}$ mice and $Itgb7^{+/+}Il10^{-/-}$ mice (Figure 3*A* and *B*), indicating that Tregs generally were not reduced in the absence of $\beta7$. A similar reduction in colonic lamina propria Tregs was observed in piroxicam-treated $Itgb7^{-/-}Il10^{-/-}$ mice (Figure 3*C*). Importantly, expression of canonical Treg markers CD25 and Foxp3 was similar in $Itgb7^{-/-}Il10^{-/-}$ mice and $Itgb7^{+/+}Il10^{-/-}$ mice (Figure 4). Furthermore, a wide variety of other Treg-associated proteins including OX40, CD152, T-bet, GATA3, and KLRG1 were expressed at similar levels in Tregs from spleen and lamina propria of $Itgb7^{-/-}Il10^{-/-}$ mice and $Itgb7^{+/+}Il10^{-/-}$ mice (Figure 5). As expected, CD103 (αE), which requires pairing with $\beta7$, is not expressed in $Itgb7^{-/-}Il10^{-/-}$ Tregs (Figure 5). In sum, these data show that integrin $\beta7$ deficiency results in a profound reduction of

colonic Tregs in *Itgb7*$^{-/-}$*Il10*$^{-/-}$ mice. Moreover, the number of Tregs in mesenteric lymph nodes (MLNs) also was reduced significantly in *Itgb7*$^{-/-}$*Il10*$^{-/-}$ mice. However, the Treg numbers in peripheral lymph nodes (PLNs) was similar to *Itgb7*$^{+/+}$*Il10*$^{-/-}$ mice (Figure 6). Thus, in this colitis model, the absence of β7 causes a profound reduction

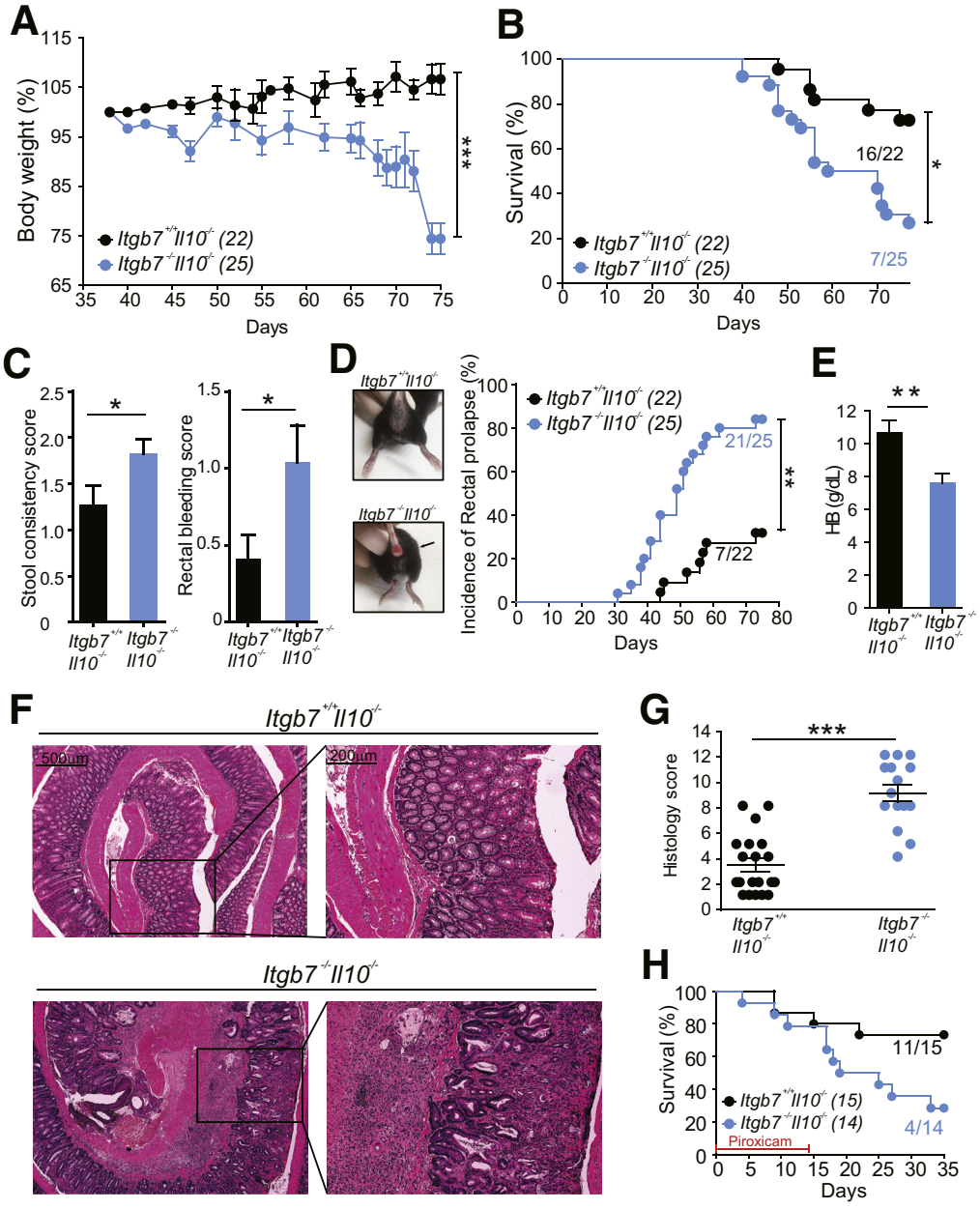

Figure 1. Loss of β7 expression exacerbated spontaneous colitis induced by IL10 deficiency. Changes in (*A*) body weight, (*B*) survival ratio, (*C*) stool consistency and rectal bleeding, and (*D*) rectal prolapse occurrence in *Itgb7*$^{+/+}$*Il10*$^{-/-}$ mice (n = 22) and *Itgb7*$^{-/-}$*Il10*$^{-/-}$ mice (n = 25). Changes in body weight are shown as a percentage of the original weight. The stool consistency score was as follows: 0 (normal), 1 (soft), 2 (very soft), and 3 (diarrhea); the rectal bleeding score was as follows: 0 (none), 1 (red), 2 (dark red), and 3 (gross bleeding). Data represent means ± SEM. Two-way analysis of variance with the Bonferroni posttest. (*E*) Concentration of hemoglobin in peripheral blood from *Itgb7*$^{+/+}$*Il10*$^{-/-}$ mice (n = 20) and *Itgb7*$^{-/-}$*Il10*$^{-/-}$ mice (n = 15) at day 75 are shown. The concentration of hemoglobin in peripheral blood from *Itgb7*$^{+/+}$*Il10*$^{+/+}$ mice was approximately 13–14 g/dL. Data represent means ± SEM. Two-tailed *t* test. (*F* and *G*) Representative H&E staining of Swiss rolls of distal colon sections from *Itgb7*$^{+/+}$*Il10*$^{-/-}$ mice (n = 20) and *Itgb7*$^{-/-}$*Il10*$^{-/-}$ mice (n = 15) at day 75. (*F*) *Scale bars*: 500 μm. (*G*) Histology score was as described in the Material and Methods section. Data represent means ± SEM. Two-tailed *t* test. (*H*) Survival ratio of *Itgb7*$^{+/+}$*Il10*$^{-/-}$ mice (n = 15) and *Itgb7*$^{-/-}$*Il10*$^{-/-}$ mice (n = 14) after piroxicam treatment (200 ppm) for 2 weeks. Data represent means ± SEM. Two-way analysis of variance with the Bonferroni posttest. *, .01< *P* < .05; **, .001< *P* < .01; ***, *P* < .001. WT, *Itgb7*$^{+/+}$*Il10*$^{-/-}$ mice; *Itgb7*$^{-/-}$, *Itgb7*$^{-/-}$*Il10*$^{-/-}$ mice. (*E* and *G*) Data include surviving mice from panel *A* and additional mice that were not assessed for daily weights.

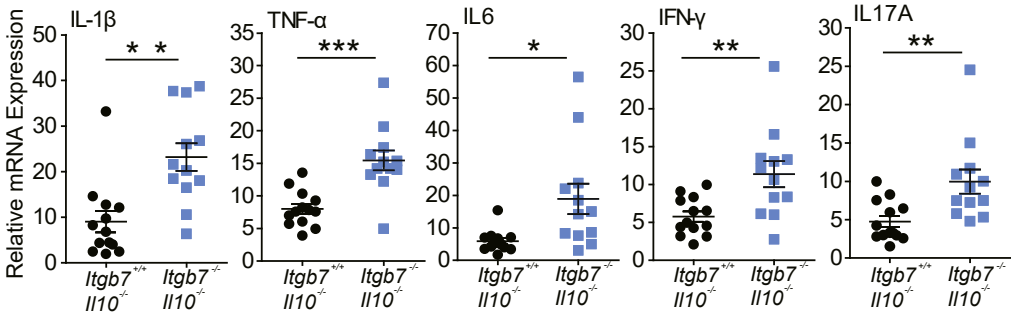

Figure 2. RNA expression of cytokines in *Itgb7*$^{+/+}$*Il10*$^{-/-}$ mice and *Itgb7*$^{-/-}$ *Il10*$^{-/-}$ mice. Messenger RNA (mRNA) expression of IL1β, tumor necrosis factor (TNF)-α, IL6, interferon (IFN)γ, and IL17A in distal colon tissue from *Itgb7*$^{+/+}$*Il10*$^{-/-}$ mice (n = 13) and *Itgb7*$^{-/-}$*Il10*$^{-/-}$ mice (n = 12). Results are normalized to glyceraldehyde-3-phosphate dehydrogenase. Data represent means ± SEM. Two-tailed *t* test. **P* < .01, ***P* < .01, ****P* < .001. WT, *Itgb7*$^{+/+}$*Il10*$^{-/-}$mice; *Itgb7*$^{-/-}$, *Itgb7*$^{-/-}$*Il10*$^{-/-}$ mice.

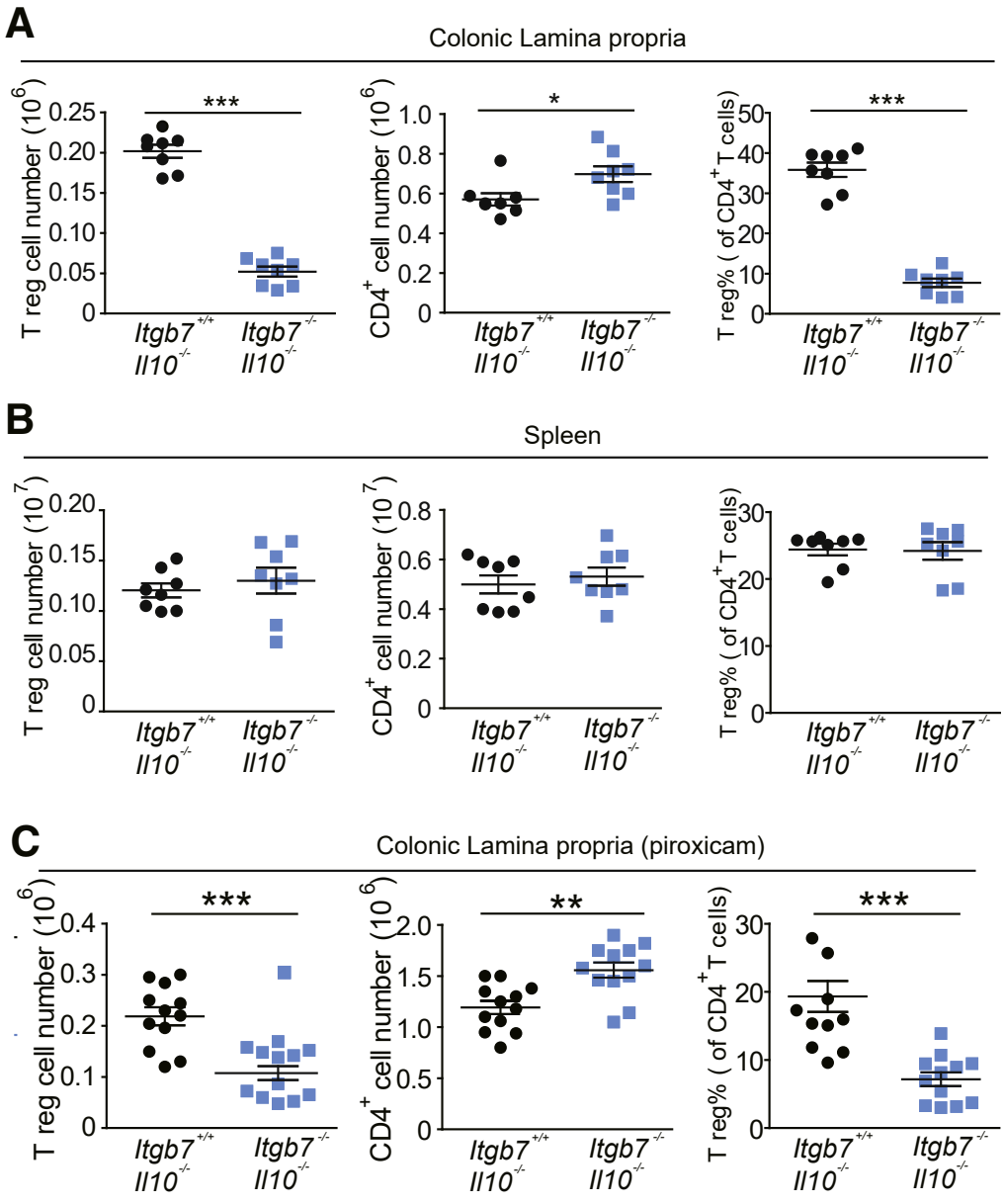

Figure 3. Loss of β7 expression impaired migration of Tregs to the colon in IL10-deficient mice. (*A* and *B*) Number and percentage of Tregs in CD4$^+$ T cells in (*A*) colonic lamina propria and (*B*) spleen from *Itgb7*$^{+/+}$*Il10*$^{-/-}$ mice (n = 8) and *Itgb7*$^{-/-}$*Il10*$^{-/-}$ mice (n = 8). (*C*) Number and percentage of Tregs in CD4$^+$ T cells in colonic lamina propria from *Itgb7*$^{+/+}$*Il10*$^{-/-}$ mice (n = 12) and *Itgb7*$^{-/-}$*Il10*$^{-/-}$ mice (n = 12) after piroxicam treatment (200 ppm) for 2 weeks. Data represent means ± SEM. Two-tailed *t* test. **P* < .05, ***P* < .01, ****P* < .001. WT, *Itgb7*$^{+/+}$*Il10*$^{-/-}$ mice; *Itgb7*$^{-/-}$, *Itgb7*$^{-/-}$*Il10*$^{-/-}$ mice.

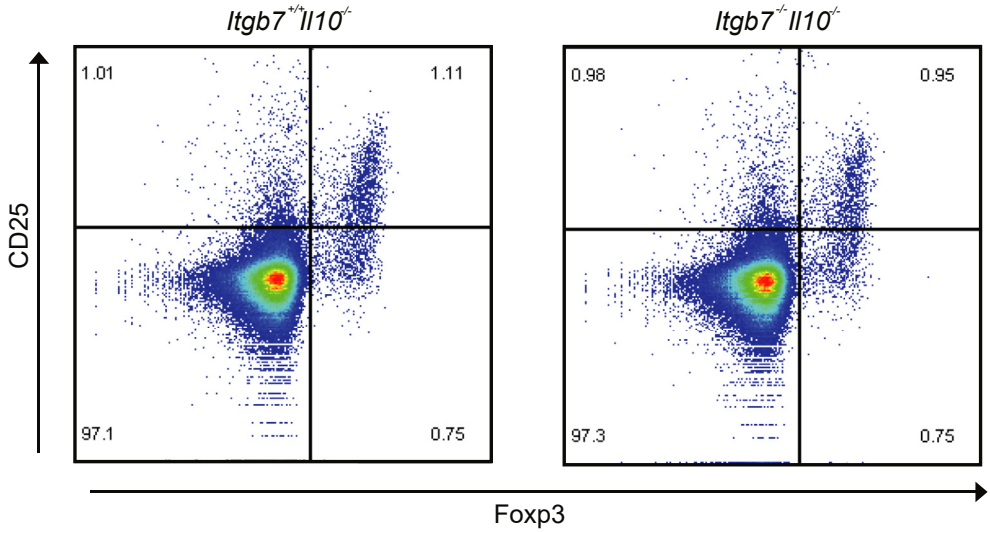

Figure 4. CD25 and Foxp3 expression on *Itgb7*$^{-/-}$ Tregs. Expression of CD25 and Foxp3 on Tregs from *Itgb7*$^{+/+}$*Foxp3*^{GFP} or *Itgb7*$^{-/-}$*Foxp3*^{GFP} mice are shown. Splenocytes were stained with CD25 antibody and then analyzed by flow cytometry.

of Tregs in GALT; however, with the exception of αEβ7, β7-null Tregs that enter the colon express a typical repertoire of Treg-associated markers and transcription factors.

Integrin β7–Deficient CD4$^+$ T Cells Ameliorate Adoptive T-Cell–Transfer–Induced Colitis

The foregoing results led us to ask whether the deleterious effects of loss of β7 function were mediated by effects on Tconv or Tregs. To investigate the role of β7 in Tconv cells and their capacity to induce colitis, we transferred CD4$^+$CD25$^-$CD45RB^{high} T cells (Tconv cells) from wild-type (WT) mice or *Itgb7*$^{-/-}$ mice into *Rag1*$^{-/-}$ recipient mice. *Rag1*$^{-/-}$ mice injected with WT Tconv cells showed a dramatic loss in body weight starting at 20–30 days, and one third of the mice died by 90 days (Figure 7*A* and *B*). In contrast, *Rag1*$^{-/-}$ mice injected with *Itgb7*$^{-/-}$ Tconv cells showed a significantly milder and delayed weight loss compared with WT Tconv cells and most of the mice survived (Figure 7*A* and *B*).

We next tested the role of integrin β7 on CD4$^+$ T-cell migration using the competitive homing assay. β7-deficient CD4$^+$ T cells were impaired for homing to MLNs and Peyer's patch (PP), but not PLNs and spleen (SP) (Figure 7*C*), which is consistent with previous studies.[33] Thus, β7-deficient CD4$^+$ T cells manifest a defective migration to the colon, which reduces adoptive T-cell–transfer–induced colitis.

Integrin β7-Deficient Tregs Are Defective in the Capacity to Prevent Colitis

We examined the effect of β7 deficiency on the ability of Tregs to prevent intestinal inflammation in the adoptive T-cell transfer model.[34] Transfer of CD4$^+$CD25$^-$CD45RB^{high} T cells (CD4$^+$ Tconv) into *Rag1*$^{-/-}$ mice led to a severe colitis by 6–12 weeks after cell transfer. Loss of body weight started after 20 days (Figure 8*A*), and half of the mice had died by 90 days (Figure 8*B*). As expected, co-injection of *Itgb7*$^{+/+}$ Tregs with Tconv prevented colitis (Figure 8*A* and *B*), whereas injection of *Itgb7*$^{-/-}$ Tregs with Tconv did not prevent disease. At 90 days, the disease markers in the mice receiving co-administered β7-deficient Tregs was similar to that of those receiving only Tconv (Figure 8*C* and *D*). Moreover, expression of proinflammatory cytokines in the colon was not significantly different in mice receiving *Itgb7*$^{-/-}$ Tregs compared with Tconv alone, whereas those that had received *Itgb7*$^{+/+}$ Tregs showed only minimal cytokine expression (Figure 8*E*). These results show that β7 deficiency impairs the capacity of Tregs to prevent adoptive T-cell–transfer–induced colitis, whereas it impairs the capacity of Tconv to cause colitis.

Defective Suppression of Colitis in β7-Deficient Tregs Is Ascribable to Defective Homing

To evaluate the possibility that integrin β7-deficient Tregs lacked suppressive capacity we examined their ability to inhibit T-cell proliferation. Green fluorescent protein positive (GFP$^+$) Tregs were sorted from *Itgb7*$^{+/+}$*Foxp3*^{GFP} or *Itgb7*$^{-/-}$*Foxp3*^{GFP} mice and their capacity to suppress proliferation of CD4$^+$CD25$^-$ responder cells was compared in a dye dilution assay. Carboxyfluorescein succinimidyl ester (CFSE)-labeled responder cells stimulated with immobilized anti-CD3 and anti-CD28 in the presence of IL2 for 4 days at 37°C proliferated vigorously as indicated by the dilution of fluorescence (Figure 9*A*). The addition of a 1:1 ratio of β7-deficient or replete Tregs markedly reduced proliferation in these cultures (Figure 9*A*). The proliferation index as a function of Treg/responder ratio was not significantly different between cultures with Treg lacking β7 and those sufficient for β7 (Figure 9*B*). Furthermore, β7-deficient Tregs showed similar expression of the anti-inflammatory cytokines IL10 and transforming growth factor (TGF)-β1 as wild-type Tregs (Figure 9*C*). Thus, β7-deficient Tregs are functionally intact with regard to their suppressive functions.

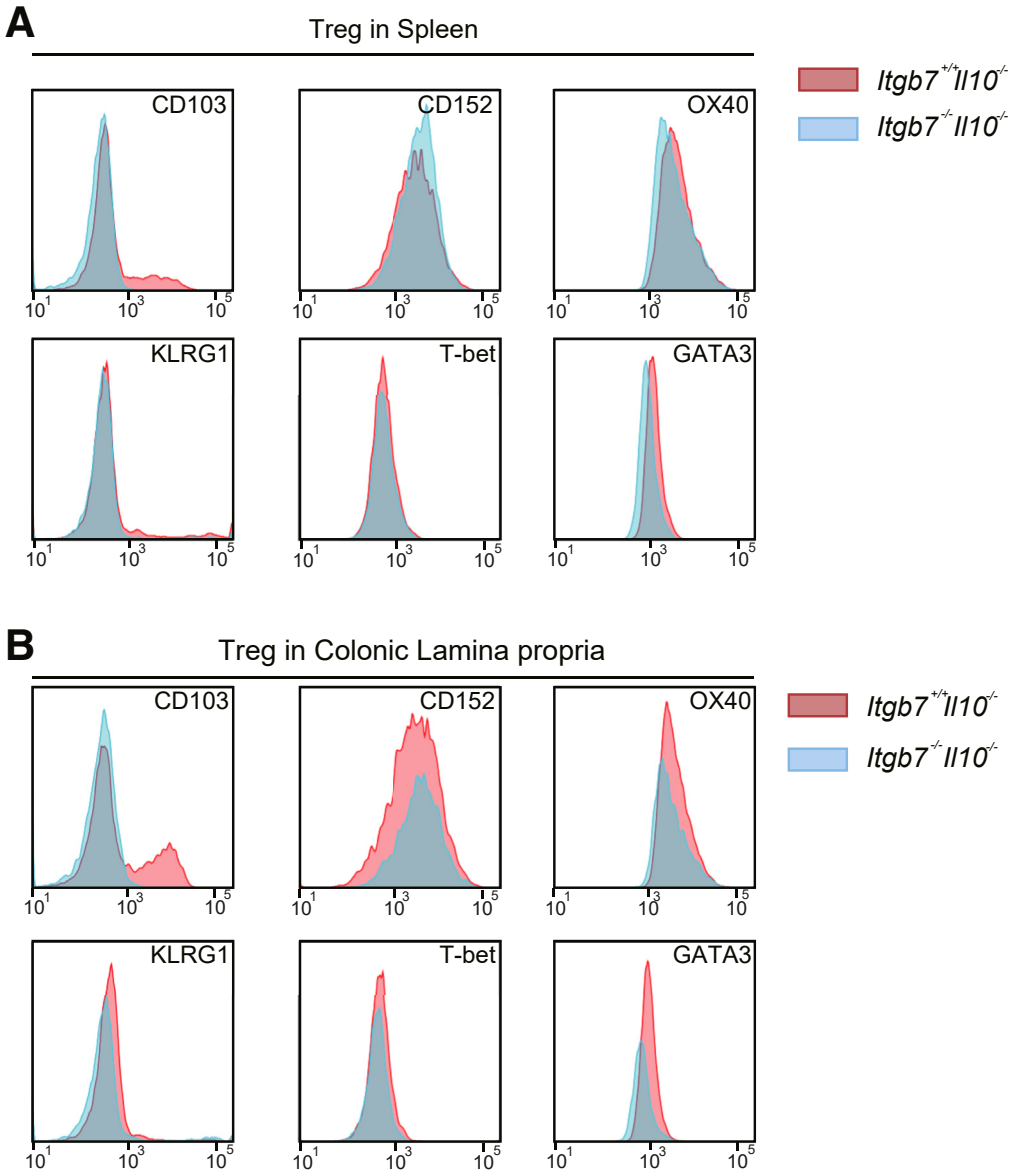

Figure 5. Treg markers and transcription factor expression on *Itgb7*$^{-/-}$ Tregs. Expression of Treg markers CD103, CD152 (CTLA4), OX40, and KLRG1, as well as transcription factors T-bet and GATA3, are shown. Cells from (*A*) spleen and (*B*) colonic lamina propria were isolated, stained with the indicated antibody, and then analyzed by flow cytometry.

The failure of *Itgb7*$^{-/-}$ Tregs to efficiently suppress colitis despite normal intrinsic suppressive function suggested that defective homing of *Itgb7*$^{-/-}$ Tregs may explain their reduced capacity to block colon inflammation. To test this idea, we used a competitive homing assay with GFP^{+} Tregs isolated from *Itgb7*$^{+/+}$*Foxp3*^{GFP} or *Itgb7*$^{-/-}$*Foxp3*^{GFP} mice, labeled them with a 1 μmol/L and 10 μmol/L concentration of eFluor670 proliferation dye, respectively, and co-injected equal numbers (1×10^7) of differentially labeled cells into recipient mice. Lymphoid organs were harvested 3 hours after injection, and cells were isolated and analyzed by flow cytometry. Similar to the known effects of deficiency on Tconv homing (Figure 7*C*), β7-deficient Tregs homing to PP was reduced by approximately 90% compared with β7-sufficient cells, whereas homing to MLN was reduced modestly (~50%). In contrast, homing of Tregs to PLN and SP were similar in *Itgb7*$^{-/-}$ and *Itgb7*$^{+/+}$ Tregs (Figure 9*D*). The absolute cell numbers of both WT or Itgb7$^{-/-}$ Tregs in the different organs also were checked (Figure 10). Thus, there is a profound reduction in Tregs in the GALT of *Itgb7*$^{-/-}$ mice that is attributable, at least in part, to defective homing of these cells, and this reduction can account for the exacerbation of colitis on an *Il10*$^{-/-}$ background.

β7 Deficiency Does Not Exacerbate Acute Dextran Sulfate Sodium–Induced Colitis

Increased colitis in *Itgb7*$^{-/-}$*Il10*$^{-/-}$ mice seemed paradoxic in light of the therapeutic efficacy of α4β7 blockade in IBD patients. We reasoned that the combination of reduced functionality of Tregs lacking IL10 combined with a reduction of Tregs in the GALT of β7-deficient mice might synergistically reduce Treg function in the gut sufficient to exacerbate colitis. To test this idea, we examined the effect

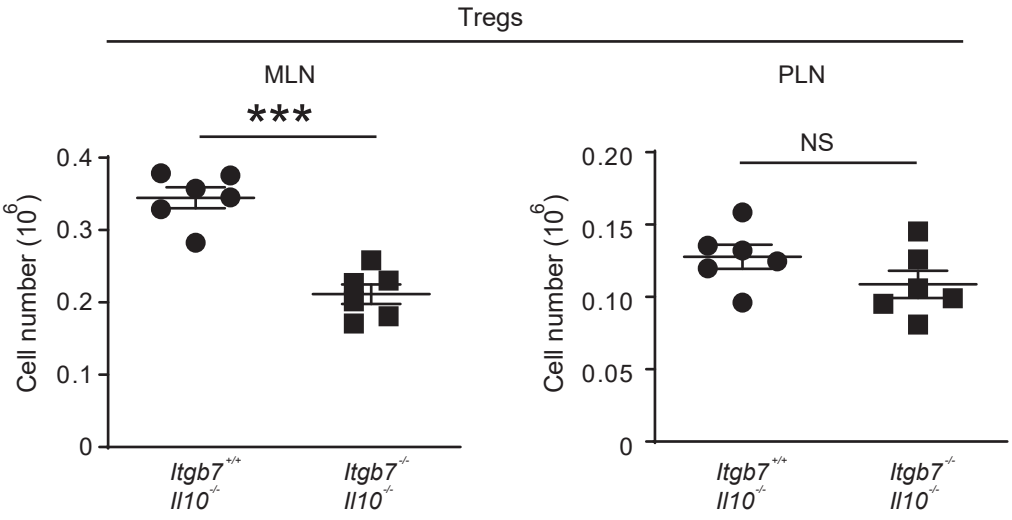

Figure 6. Loss of β7 expression on migration of Tregs to the MLN in IL10-deficient mice. The number of Tregs in MLN and PLN from *Itgb7*$^{+/+}$*Il10*$^{-/-}$ mice (n = 6) and *Itgb7*$^{-/-}$*Il10*$^{-/-}$ mice (n = 6) Data represent means ± SEM. One-way analysis of variance with the Bonferroni posttest. ***$P < .001$.

of β7 deficiency in a colitis model in which Treg function was normal. We administered dextran sulfate sodium (DSS) for 7 days and then analyzed the mice for an additional 7 days, times at which inflammation is dominated largely by the innate immune response to bacterial products that breach the intestinal barrier as a consequence of mucosal injury.[31,35] Subsequently, an adaptive immune component can contribute to further chronic inflammation,[36] thus potentially accounting for the finding by Zhang et al that β7 deficiency exacerbated a later stage of DSS colitis.[28] Both *Itgb7*$^{+/+}$ and *Itgb7*$^{-/-}$ mice showed similar rapid body weight loss during the initial phase of DSS treatment. Once DSS administration was halted, *Itgb7*$^{-/-}$ mice gained weight slightly but significantly more rapidly than *Itgb7*$^{+/+}$ mice (Figure 11*A*). *Itgb7*$^{-/-}$ mice showed less mucosal immune cell infiltration and crypt destruction (Figure 11*B*), as shown by lower histologic scores (Figure 11*C*), and further supported by less anemia (Figure 6*D*). Thus, in sharp contrast to the IL10-deficient model, β7 deficiency did not exacerbate inflammation in this acute DSS model of colitis.

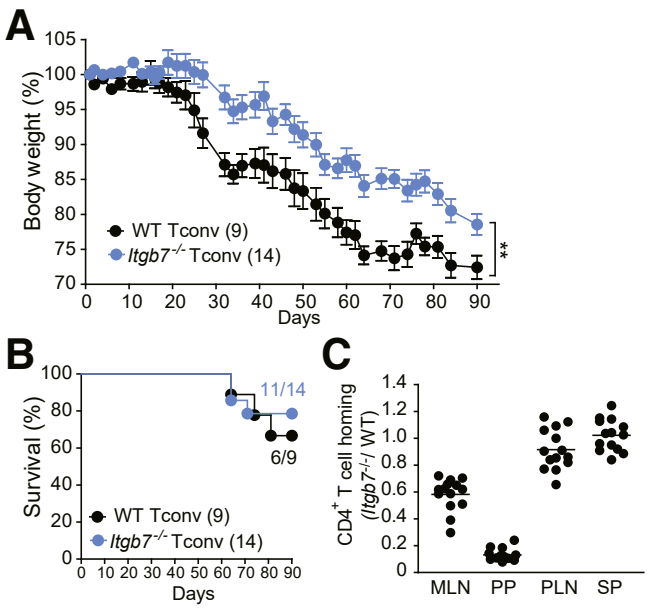

Figure 7. β7-deficient CD4$^+$ T cells ameliorate adoptive T-cell–transfer–induced colitis. (*A* and *B*) CD4$^+$CD25$^-$CD45RB^{high} Tconv cells (1 × 10^6) from *Itgb7*$^{+/+}$ or *Itgb7*$^{-/-}$ mice were injected into *Rag1*$^{-/-}$ mice. Changes in (*A*) body weight and (*B*) survival ratio are shown. Changes in body weight are shown as a percentage of the original weight. The number of mice in each group is indicated. Data represent means ± SEM. Two-way analysis of variance with the Bonferroni posttest. (*C*) In vivo competitive homing of CD4$^+$ T cells to lymphoid tissues. CD4$^+$ T cells were isolated from either *Itgb7*$^{+/+}$ or *Itgb7*$^{-/-}$ mice, differentially labeled, and mixed before injection into C57BL/6 mice. CD4$^+$ T cells homing to different lymphoid organs were analyzed by flow cytometry 3 hours after injection. The ratio of *Itgb7*$^{-/-}$ CD4$^+$ T cells to *Itgb7*$^{+/+}$ CD4$^+$ T cells (*Itgb7*$^{-/-}$/WT) from different lymphoid organs is shown ($n = 14$). Data represent means ± SEM. One-way analysis of variance with the Bonferroni posttest. **$P < .01$. WT Tconv, Tconv cells from *Itgb7*$^{+/+}$ mice; *Itgb7*$^{-/-}$ Tconv, Tconv cells from *Itgb7*$^{-/-}$ mice.

Antibody Blockade of α4β7–MAdCAM-1 Interaction Aggravates Spontaneous Colitis Induced by IL10 Deficiency

The foregoing studies showed that genetic inactivation of integrin β7 exacerbated colitis in *Itgb7*$^{-/-}$*Il10*$^{-/-}$ mice and ascribed the exacerbation to a combination of reduced Treg function and homing to GALT. These results raise 2 important issues: (1) β7 can combine with αE or α4; can loss of only α4β7 function exacerbate colitis in IL10-null mice? (2) *Itgb7*$^{-/-}$ mice lack β7 function throughout development: will loss of α4β7 function in an adult IL10-deficient mouse exacerbate colitis? MAdCAM-1, which is expressed preferentially on gut and GALT-associated endothelial cells, plays a vital role in α4β7-mediated leukocyte trafficking to the GALT and is a primary ligand of integrin α4β7. Because we did not have access to a function blocking antimurine α4β7, *Il10*$^{-/-}$ mice

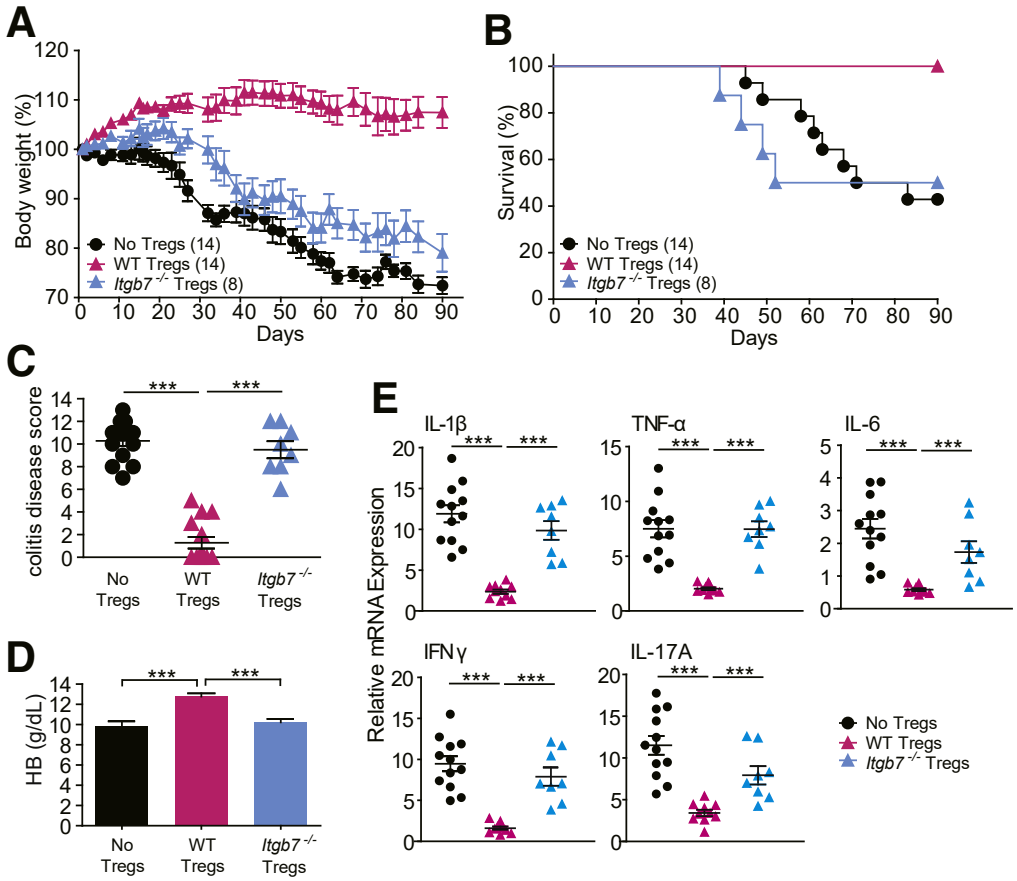

Figure 8. Reduced ability of β7-null Tregs to prevent adoptive T-cell–transfer–induced colitis. $CD4^+CD25^-CD45RB^{high}$ Tconv cells (1×10^6) isolated from C57BL/6 mice were injected into *Rag1*$^{-/-}$ mice in the presence or absence of 2×10^5 $CD4^+CD25^+CD45RB^{low}$ Tregs isolated from *Itgb7*$^{+/+}$ or *Itgb7*$^{-/-}$ mice. Changes in (*A*) body weight and (*B*) survival ratio are shown. Changes in body weight are shown as a percentage of the original weight. The number of mice in each group is indicated. Data represent means ± SEM. Two-way analysis of variance with the Bonferroni posttest. (*C*) The colitis disease score is shown. Data represent means ± SEM. One-way analysis of variance with the Bonferroni posttest. (*D*) The concentration of hemoglobin in peripheral blood from each group at day 90 is shown. Data represent means ± SEM. Two-tailed *t* test. (*E*) Messenger RNA (mRNA) expression analysis of IL1β, tumor necrosis factor (TNF)-α, IL6, interferon (IFN)γ, and IL17A in distal colon tissue. Results are normalized to glyceraldehyde-3-phosphate dehydrogenase. Data represent means ± SEM. One-way analysis of variance with the Bonferroni posttest. ***$P < .001$. No Tregs, only Tconv cells; WT Tregs, Tconv cells plus WT Tregs; *Itgb7*$^{-/-}$ Tregs, Tconv cells plus *Itgb7*$^{-/-}$ Tregs.

were treated with a MAdCAM-1 blocking antibody, MECA367, which inhibits binding of α4β7 integrin to MAdCAM-1[37] and ameliorates DSS-induced colitis.[38,39] MECA367-treated *Il10*$^{-/-}$ mice showed profound weight loss and shorter survival compared with control IgG-treated *Il10*$^{-/-}$ mice (Figure 12*A* and *B*). Furthermore, MECA367-treated *Il10*$^{-/-}$ mice showed more severe anemia (Figure 12*C*) and increased inflammation and colonic tissue injury (Figure 12*D* and *E*) compared with control IgG-treated *Il10*$^{-/-}$ mice. Thus, blocking the interaction between MAdCAM-1 and integrin α4β7 in vivo aggravates spontaneous colitis induced by IL10 deficiency.

Discussion

Leukocyte homing to GALT has complex roles in the pathogenesis of IBD.[15,40–42] Antibodies against β7 integrins, which inhibit leukocyte trafficking to the gut and GALT, are not uniformly efficacious at ameliorating IBD.[15] Here, we report that mice lacking IL10, a major immunosuppressive cytokine of Tregs, unexpectedly developed increased intestinal inflammation when β7 was genetically inactivated or α4β7-mediated GALT homing was blocked by antibodies. These effects of loss of β7 function were associated with reduced Tregs in the lamina propria owing to impaired Treg homing to the gut. In an adoptive transfer model of intestinal inflammation, we found that β7-deficient Tregs are impaired in their capacity to colonize GALT and to oppose intestinal inflammation despite possessing normal intrinsic suppressive functions. We propose that the combination of reduced Treg function in IL10-null mice and reduced Treg homing owing to loss of β7 function, in combination, decrease net Treg suppressive activity in the gut sufficiently to counteract the protective effect of blocking β7 on homing of conventional T cells. Thus, Treg numbers or functions could affect the efficacy of β7 blockade in IBD (Figure 13).

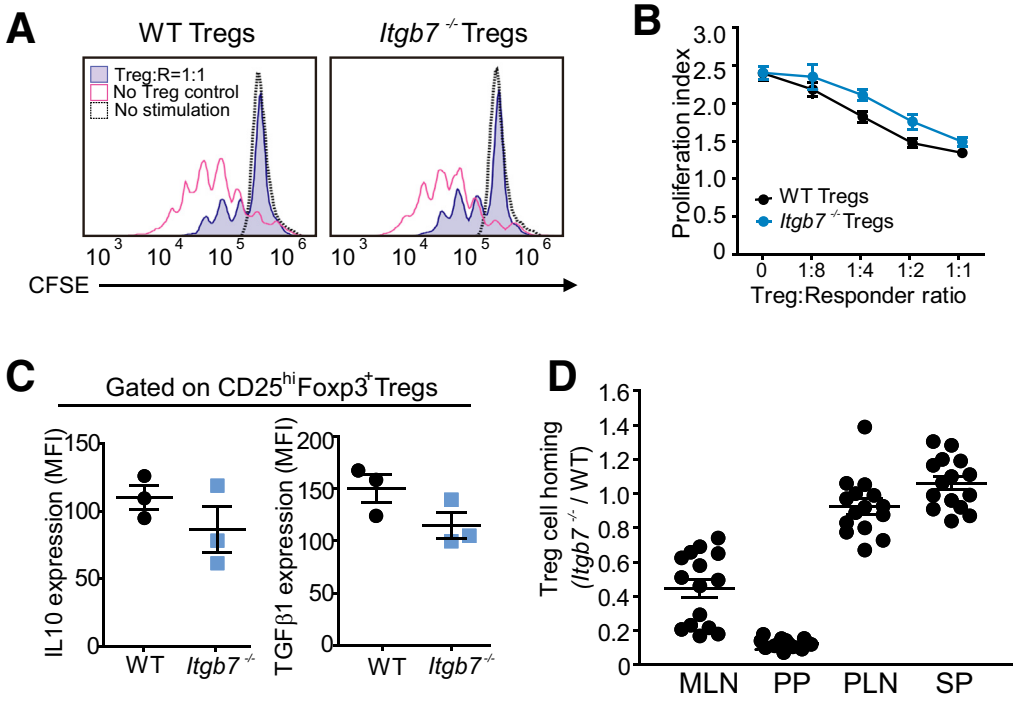

Figure 9. β7-deficient Tregs show normal suppression in vitro. (*A* and *B*) Treg suppression function. Tregs isolated from CD45.2 congenic *Itgb7*$^{+/+}$*Foxp3*^{GFP} (WT Treg) or *Itgb7*$^{-/-}$*Foxp3*^{GFP} (*Itgb7*$^{-/-}$ Treg) mice were mixed with responder cells at the indicated Treg/responder cell ratios. Responder cells are CFSE-labeled CD45.1 congenic C57BL/6 CD4^{+}CD25^{-} conventional T cells activated by anti-CD3 (5 μg/mL), anti-CD28 (5 μg/mL), and IL2. (*A*) CFSE populations gated on CD45.1^{+} cells were analyzed by flow cytometry at 72 hours. (*B*) The proliferation index was determined by FlowJo software. (*C*) Intracellular expression of IL10 and TGFβ1 of GFP^{+} Tregs from *Itgb7*$^{+/+}$*Foxp3*^{GFP} (WT) or *Itgb7*$^{-/-}$*Foxp3*^{GFP} (*Itgb7*$^{-/-}$) mice. Splenocytes were stimulated ex vivo with phorbol myristate acetate and ionomycin in the presence of monensin (for IL10) or brefeldin A (for TGF-β1) for 4 hours at 37°C. Cells were fixed and permeabilized before staining (n = 3). Data represent means ± SEM. Two-tailed *t* test. (*D*) In vivo competitive homing of Tregs to different lymphoid tissues. GFP^{+} Tregs were sorted from *Itgb7*$^{+/+}$*Foxp3*^{GFP} (WT) or *Itgb7*$^{-/-}$*Foxp3*^{GFP} (*Itgb7*$^{-/-}$) mice. Lymphoid organs were isolated 3 hours after injection of Tregs before flow cytometry analysis. The ratio of *Itgb7*$^{-/-}$ Tregs to *Itgb7*$^{+/+}$ Tregs (*Itgb7*$^{-/-}$/WT) within various lymphoid tissues is shown (*n* = 15). Data represent means ± SEM. One-way analysis of variance with the Bonferroni posttest. WT Tregs, Tregs from *Itgb7*$^{+/+}$*Foxp3*^{GFP}mice; *Itgb7*$^{-/-}$ Tregs, Tregs from *Itgb7*$^{-/-}$*Foxp3*^{GFP}mice. MFI, mean fluorescence intensity.

Surprisingly, loss of β7 function in mice lacking IL10 caused increased intestinal inflammation. Genetic β7 deficiency aggravated spontaneous colitis in IL10-deficient mice as judged by dramatic body weight loss accompanied by severe diarrhea and rectal bleeding. These symptoms were associated with histologic evidence of increased tissue damage and inflammation, worsened anemia, and increased colonic expression of proinflammatory cytokines. Importantly, because we were obliged to breed *Il10*$^{-/-}$ mice through crosses of *Il10*$^{+/-}$ mice, it was not feasible to generate sufficient numbers of littermate *Itgb7*$^{-/-}$*Il10*$^{-/-}$ and *Itgb7*$^{+/+}$ *Il10*$^{-/-}$ controls. Because β7 deficiency can impact the intestinal flora,[43] even though β7-null and WT mice were on a C57 BL/6 background and were cohoused, it is possible that some of the effects of β7 deficiency could be the result of an altered microbiome. That said, *Il10*$^{-/-}$ mice experienced a similar worsening of colitis after antibody blockade of α4β7–MAdCAM-1 interaction in comparison with cohoused IgG-treated littermates. Furthermore, in the adoptive transfer model of colitis, we documented that β7-null Tregs were defective in suppressing intestinal inflammation compared with WT Tregs when administered to cohoused littermate mice. These results sharply contrast with the beneficial effects of α4β7-blocking antibody in patients with active UC or CD.[15,16] Earlier studies in mice also reported that inhibiting β7-integrin function attenuated acute and chronic murine models of intestinal inflammation.[44,45] Thus, loss of β7 integrin function causes increased intestinal inflammation in IL10-deficient mice despite its often beneficial effects in other murine models and in human beings with IBD.

Vedolizumab blocks integrin α4β7 on both effector T cells and Tregs. Recent studies have reported that α4β7 is crucial for controlling homing of Tregs in patients with UC to the inflamed colon in vivo,[29] and β7 deficiency causes Treg depletion in the gut.[30,31] Nevertheless, our data suggest that combined loss of Treg function and β7-dependent Treg homing to gut and GALT together can counteract a protective effect of β7 blockade of effector T-cell migration on intestinal inflammation. Integrin *Itgb7*$^{-/-}$ Tregs were defective in their capacity to prevent induction of colitis in immune-deficient mice reconstituted with Tconv. We note that Denning et al reported that *Itgb7*$^{-/-}$ Tregs could prevent colitis in their adoptive transfer model, a difference that might be a consequence of their use of a different

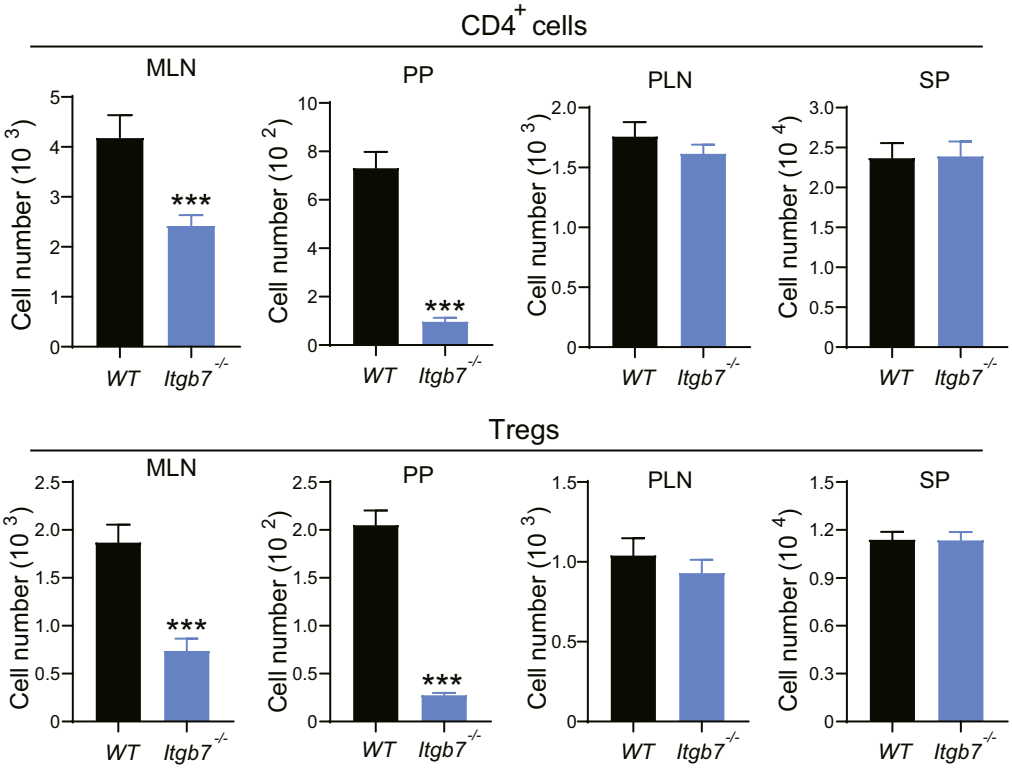

Figure 10. Cell number of homed Tregs in different organs in the competitive homing assay. In vivo competitive homing of (*A*) $CD4^+$ T cells or (*B*) Tregs to lymphoid tissues. (*A*) $CD4^+$ T cells or (*B*) Tregs were isolated from either WT or *Itgb7*$^{-/-}$ mice, differentially labeled and mixed before injection into C57BL/6 mice. The absolute cell numbers of WT or *Itgb7*$^{-/-}$ (*A*) $CD4^+$ T cells or (*B*) Tregs in different lymphoid organs was shown ($n = 14$). Data represent means ± SEM. One-way analysis of variance with the Bonferroni posttest. ***$P < .001$. WT, *Itgb7*$^{+/+}$ mice; *Itgb7*$^{-/-}$, *Itgb7*$^{-/-}$ mice.

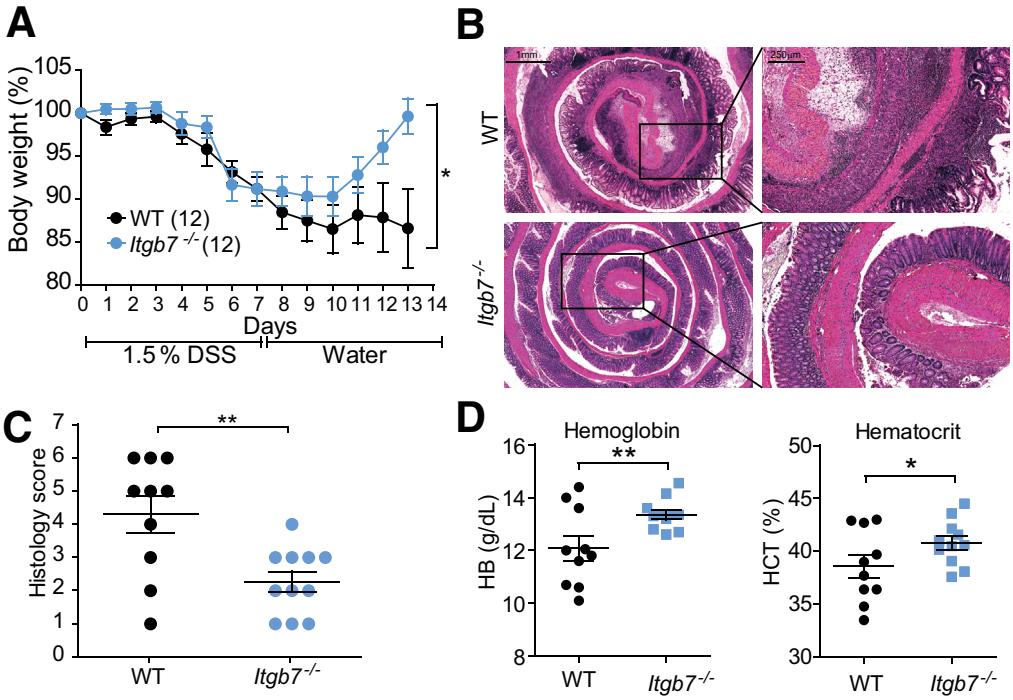

Figure 11. β7 deficiency does not exacerbate DSS-induced acute colitis. Eight-week-old *Itgb7*$^{+/+}$ and *Itgb7*$^{-/-}$ mice were treated with 1.5% DSS for 7 days, followed by regular drinking water. (*A*) Changes in body weight are shown as a percentage of the original weight. Data represent means ± SEM. Two-way analysis of variance with the Bonferroni posttest. (*B*) Representative H&E staining of Swiss rolls of distal colon sections at day 14. Scale bars are labelled in the images. (*C*) Histology score was determined as described in the Materials and Methods section. (*D*) Hemoglobin concentration and hematocrit in peripheral blood from *Itgb7*$^{+/+}$ and *Itgb7*$^{-/-}$ mice at day 14 are shown. Data represent means ± SEM. Two-tailed *t* test. *$P < .05$, **$P < .01$. WT, *Itgb7*$^{+/+}$ mice; *Itgb7*$^{-/-}$, *Itgb7*$^{-/-}$ mice.

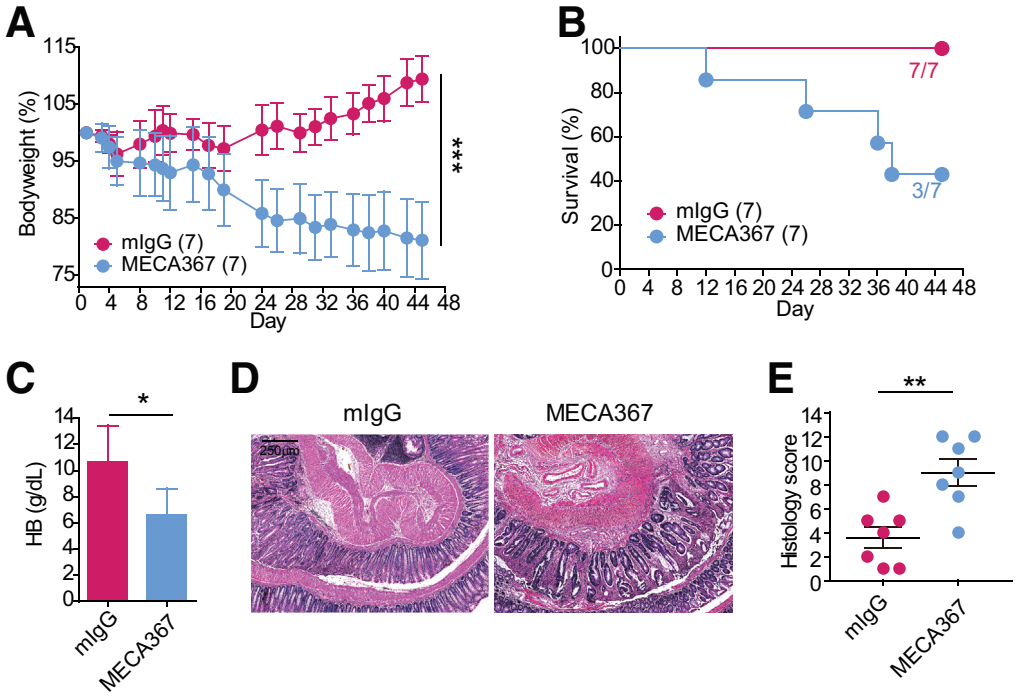

Figure 12. Blocking MAdCAM-1 interaction with α4β7 integrin worsened spontaneous colitis induced by IL10 deficiency. The IL10-deficient mice were injected intraperitoneally with anti–MAdCAM-1 blocking antibody MECA367 (100 μg/mouse) every 4 days. (*A* and *B*) Changes in (*A*) body weight and (*B*) survival ratio of murine IgG control- or MECA367-treated IL10-deficient mice. Changes in body weight are shown as a percentage of the original weight. Data represent means ± SEM. Two-way analysis of variance with the Bonferroni posttest. (*C*) Concentration of hemoglobin (HB) in peripheral blood at day 45 posttreatment is shown. Data represent means ± SEM. Two-tailed *t* test. (*D* and *E*) Representative H&E staining of Swiss rolls of distal colon sections from murine IgG control- or MECA367-treated IL10-deficient mice. (*D*) *Scale bars*: 250 μm. (*E*) Histology score was assessed as described in the Material and Methods section. Data represent means ± SEM. Two-tailed *t* test. $^{*}P < .01$, $^{**}P < .01$, $^{***}P < .001$. mIgG, Mouse Immunoglobulin G.

immunodeficient recipient mouse strain.[30] Because *Itgb7*$^{-/-}$ Tregs manifested intact suppressor function in vitro, this defect likely was owing to their reduced ability to populate the gut and GALT, a reduction we can ascribe to reduced migration to the GALT as shown in competitive homing experiments. Furthermore, vedolizumab can block the homing of Tregs from UC patients to the inflamed gut.[29]

IL10 is a product of Tregs that is essential for the maintenance of intestinal homeostasis. It suppresses effector functions of T helper (Th)1/Th17 cells as well as natural killer cells and macrophages, thereby modulating both innate and adaptive immune responses[46] and muting pathogenic Th17 responses to pathobionts.[47] Tregs are a major source of IL10 to maintain homeostasis at the environmental interface of the intestine.[26] Thus, reduced homing of *Itgb7*$^{-/-}$ Tregs to gut and GALT, combined with a lack of IL10, together will profoundly reduce Treg suppression of inflammation in the colon. In contrast, *Itgb7*$^{-/-}$ mice did not experience an exacerbation of the acute DSS model in which Treg function was not impaired. IBD can have a variety of underlying causes such as defects in the NACHT, LRR and PYD domains-containing protein 3 (NLRP3) inflammasome[48] or defective Tregs. We show that reduced integrin β7–mediated homing in the setting of reduced loss of IL10 exacerbates intestinal inflammation. Thus, loss of IL10 expression or reduced Treg numbers or functions in

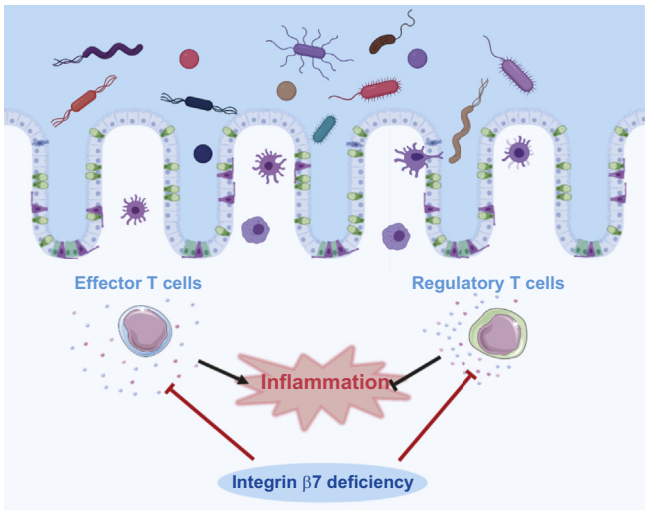

Figure 13. Schematic diagram of β7 function in gut inflammation. During gut inflammation, a disrupted protective mucus layer and epithelial barrier leads to increased uptake of luminal bacteria. Bacterial antigens result in the activation of immune cells such as T cells and macrophages, with the consequent release of proinflammatory cytokines, with further recruitment of leukocytes. β7 blockade suppresses effector T-cell migration to the gut, thereby ameliorating inflammation. However, it additionally reduced Treg homing to the gut, counteracting their anti-inflammatory activity.

patients with IBD may impact their response to therapeutic inhibition of β7 integrins.

Materials and Methods

Antibodies and Reagents

The following antibodies were from BioLegend (San Diego, CA): CD4 (GK1.5), β7 (FIB504), Foxp3 (MF-14), anti-CD3 (2C11), anti-CD28 (37.51), IL10 (JES5-16E3), TGF-β1 (TW7-16B4), and anti–MAdCAM-1 (MECA367). Secondary AlexaFluor-labeled antibodies were from Jackson ImmunoResearch (West Grove, PA). The Foxp3 transcription factor fixation/permeabilization kit was purchased from eBioscience. CFSE and eFluor670 were purchased from Invitrogen (Carlsbad, CA) and BioLegend, respectively. Piroxicam was from MilliporeSigma (Burlington, MA). Ionomycin, brefeldin A, and monensin were from BioLegend. The MojoSort mouse CD3 T-cell isolation kit and mouse CD4 T-cell isolation kit were from BioLegend. Liberase TL (research grade) and DNAse I were from Roche (Basel, Switzerland). Recombinant mouse MAdCAM-1–Fc was purified by protein A beads as previously described.[49]

Mice

All animal experiments were approved by the Institutional Animal Care and Use Committee of the University of California San Diego, and were conducted in accordance with federal regulations as well as institutional guidelines and regulations on animal studies. All mice were housed in specific pathogen-free conditions on corncob bedding and were fed ad libitum with a chow diet. C57BL/6 (CD45.1), C57BL/6 (CD45.2), *Itgb7*$^{-/-}$, *Il10*$^{-/-}$, *Rag1*$^{-/-}$ mice were from The Jackson Laboratory (Bar Harbor, ME). *Foxp3*^{GFP} mice have been described previously.[26,50] All of the mice were on a C57BL/6 background. For experiments, 8- to 12-week-old mice were used. All injections of antibodies, control IgG, Tconv, and Tregs were performed during the light cycle.

Mononuclear cells were isolated from MLN, PP, PLN, SP, and colonic lamina propria as previously described.[13,51] Cell counting with immunofluorescence cytometry was performed using an Accuri C6 Plus and FACSCalibur (BD Biosciences, San Diego, CA).

Mouse Colitis Models

Il10$^{-/-}$ mice spontaneously develop chronic IBD under specific pathogen-free conditions. The phenotypes of chronic colitis in *Il10*$^{-/-}$ mice (C57BL/6 genetic background) became more evident at 10–12 weeks. Because *Il10*$^{-/-}$ mice develop spontaneous colitis, which has negative consequences on their capacity to breed, we separately crossed the mice as *Itgb7*$^{+/+}$*Il10*$^{+/-}$ × *Itgb7*$^{+/+}$*Il10*$^{+/-}$ and *Itgb7*$^{-/-}$*Il10*$^{+/-}$ × *Itgb7*$^{-/-}$*Il10*$^{+/-}$ to generate *Itgb7*$^{+/+}$*Il10*$^{-/-}$ and *Itgb7*$^{-/-}$*Il10*$^{-/-}$, respectively. Sex-matched *Itgb7*$^{+/+}$*Il10*$^{-/-}$ and *Itgb7*$^{-/-}$*Il10*$^{-/-}$ mice were cohoused starting at 3-4 weeks after weaning. For piroxicam treatment, mice were administered piroxicam (200 ppm in their diet everyday) for 2 weeks and killed 3 weeks after the end of piroxicam treatment.[32] For the adoptive T-cell–transfer model, 8- to 10-week-old mice were used. CD4^{+}CD25^{-}CD45RB^{high} conventional T cells (5×10^5) from C57BL/6 mice were injected intraperitoneally into cohoused *Rag1*$^{-/-}$ mice in the presence or absence of 1×10^5 CD4^{+}CD25^{+}CD45RB^{low} Tregs derived from the indicated mutant genotype littermate mice (0.2 mL phosphate-buffered saline each recipient). In acute colitis experiments, cohoused *Itgb7*$^{+/+}$ or *Itgb7*$^{-/-}$ littermates were administered 1.5% (wt/vol) DSS with a molecular mass of 36–50 kilodaltons (MP Biomedicals, Irvine, CA) in drinking water for a total of 7 days (days 0–7), followed by plain drinking water (days 8–14). Mice were assessed daily for body weight, diarrhea, and bloody stool. The disease activity index and histologic damage were assessed by trained individuals blinded to the treatment groups, as reported previously.[31] For anti–MAdCAM-1 blocking antibody MECA367 treatment, the *Il10*$^{-/-}$ cohoused littermates were injected intraperitoneally with MECA367 or control IgG (100 μg/mouse) every 4 days. Mice were euthanized, and peripheral blood was collected to test hemoglobin levels. Colons were isolated for histology and quantitative polymerase chain reaction (PCR) analysis.

Mouse body weight was measured every day and values are shown as a percentage of the original weight. During the duration of the experiment, we assessed the clinical progression of colitis by daily scoring a disease activity index. The disease activity index is the combined score of body weight loss, stool consistency, and rectal bleeding and prolapse, as follows: (1) weight loss: 0 (no loss), 1 (1%–5%), 2 (5%–10%), 3 (10%–20%), and 4 (>20%); (2) stool consistency: 0 (normal),1 (soft), 2 (very soft), and 3 (diarrhea); (3) rectal bleeding: 0 (none), 1 (red), 2 (dark red), and 3 (gross bleeding); and (4) rectal prolapse: 0 (none), 1 (signs of prolapse), 2 (clear prolapse), and 3 (extensive prolapse). Mice were killed at week 15.

Histology

Formalin-fixed, paraffin-embedded, Swiss-rolled colon sections of 4-mm thickness were mounted on glass slides and followed by H&E staining or periodic acid–Schiff staining. Images were acquired with a Nanozoomer Slide Scanner (Hamamatsu Nanozoomer 2.0 HT Slide Scanner, Hamamatsu City, Japan). Blinded histologic scoring was performed by 2 investigators based on the method described previously.[52] Two different scoring schemes were used (Tables 1 and 2).

Flow Cytometry

Cells isolated from mouse tissues were washed and resuspended in Hank's balanced salt solution containing 0.1% bovine serum albumin and 1 mmol/L Ca^{2+}/Mg^{2+} and stained with conjugated antibody for 30 minutes at 4°C. Then cells were washed twice before flow cytometry analysis using an Accuri C6 Plus or FACSCalibur (BD Biosciences). Data were analyzed using FlowJo software (FlowJo, Ashland, OR). For intracellular detection of cytokines, splenocytes were stimulated ex vivo with Phorbol 12-myristate 13-acetate and ionomycin in the presence of brefeldin A and monensin for 6 hours at 37°C; cells were fixed in 4% paraformaldehyde (Electron Microscopy

Table 1. Scoring Scheme for *Il10* Mice Model

Epithelium (0–6)	
0	Normal
1	Hyperproliferation, irregular crypts, goblet cell loss
2	Mild to moderate crypt loss (10%–50%)
3	Severe crypt loss (50%–90%)
4	Complete crypt loss, surface epithelium intact
5	Small- to medium-sized ulcer (<10 crypt widths)
6	Large ulcer (>10 crypt widths)
Infiltration with inflammatory cells (0–6)	
Mucosa	
0	None
1	Mild infiltration
2	Moderate infiltration
3	Severe infiltration
Submucosa	
0	None
1	Mild to moderate infiltration and/or edema
2	Severe infiltration
Muscularis/serosa	
0	Not involved
1	Involved

NOTE. Total score range was 0 to 12.

Sciences, Hatfield, PA) and permeabilized with the Foxp3 transcription factor fixation/permeabilization kit (eBioscience) before IL10, TGF-β1, and Foxp3 staining.

Treg Suppression Assays

$CD4^+CD25^-$ T cells (responder cells) were isolated from spleens of C57BL/6 (CD45.1) WT mice by magnetic separation using the $CD4^+$ T-cell negative isolation kit (BioLegend); a biotin-conjugated anti-CD25 (PC61; BioLegend) antibody was included to deplete Tregs. GFP^+ Tregs were sorted with a FACSAria 2 (BD Biosciences) from $Itgb7^{+/+}Foxp3^{GFP}$ or $Itgb7^{-/-}Foxp3^{GFP}$ mice. Responder cells were labeled with CFSE and cocultured with Tregs (8:1, 4:1, 2:1, and 1:1 ratios) in the presence of 5 μg/mL immobilized anti-CD3 (2C11) and anti-CD28 (37.51) and *IL2* for 4 days at 37°C. The proliferation index was calculated by FlowJo v10.

In Vivo Competitive Lymphocyte Homing

The competitive homing assay used high- and low-dose cell tracker, as described.[53] GFP^+ Tregs were sorted with a FACSAria 2 (BD Biosciences) from $Itgb7^{+/+}Foxp3^{GFP}$ or $Itgb7^{-/-}Foxp3^{GFP}$ mice and labeled with 1 μmol/L and 10 μmol/L of eFluor670, resulting in readily discriminated cell populations (Figure 14). Equal numbers of differentially labeled Tregs (1×10^7) were mixed and then injected intravenously into C57BL/6 recipient mice. Lymphoid organs were harvested 3 hours after injection and isolated cells were analyzed by flow cytometry. The ratio of $Itgb7^{-/-}$ Tregs (10 μmol/L eFluor670) to $Itgb7^{+/+}$ Tregs (1 μmol/L eFluor670) from different lymphoid organs are shown. For a competitive homing assay of β7-deficient $CD4^+$ T cells, $CD4^+$ T cells were isolated by the MojoSort mouse CD4 T-cell isolation kit from $Itgb7^{+/+}$ or $Itgb7^{-/-}$ mice and labeled with 1 μmol/L of CFSE and eFluor670, respectively.

Table 2. Scoring Scheme for DSS Model

Intestinal architecture (0–3)		
	Epithelial changes	Mucosal architecture
1	Focal erosions	
2	Erosions	± Focal ulcerations
3	Erosions	Extended ulcerations ± granulation tissue ± pseudopolyps
Infiltration with inflammatory cells (0–3)		
	Severity	Extent
1	Mild	Mucosa
2	Moderate	Mucosa and submucosa
3	Marked	Transmural

NOTE. Total score range was 0 to 6.

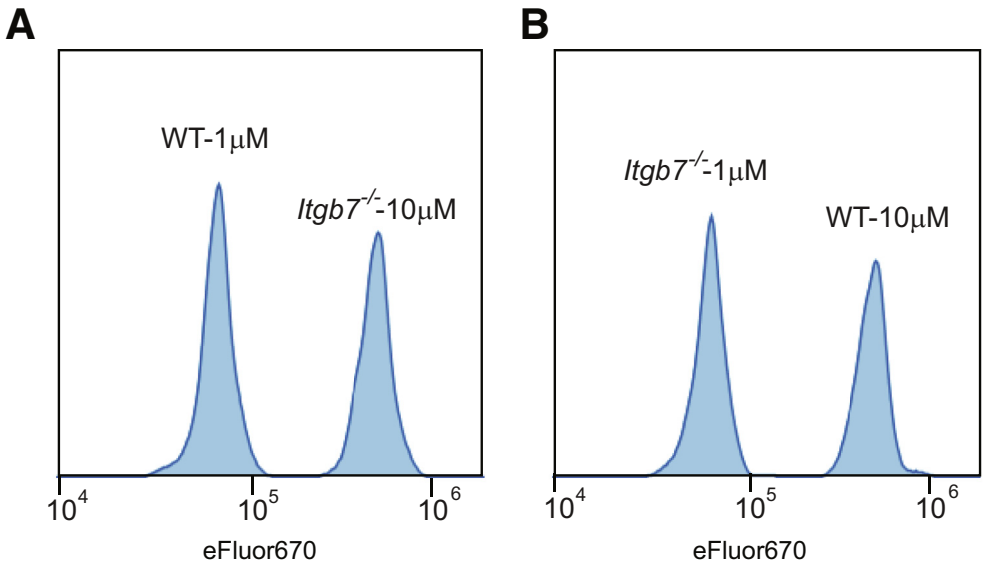

Figure 14. Validation of dual-label intensity homing assay. (*A*) GFP$^+$ Tregs were sorted with a FACSAria 2 (BD Biosciences) from *Itgb7*$^{+/+}$*Foxp3*^{GFP} or *Itgb7*$^{-/-}$*Foxp3*^{GFP} mice and labeled with 1 or 10 μmol/L of eFluor670, respectively. Equal numbers (1 X 10^7) of differentially labeled Tregs were mixed and then injected intravenously into C57BL/6 recipient mice. Spleens were harvested 3 hours after injection and isolated cells were analyzed by flow cytometry. The representative histograms were gated on GFP$^+$ Tregs. As shown in this histogram, this differential labeling produces 2 readily distinguished cell populations. (*B*) The same experiment was performed as in panel *A*, with the cell types receiving each concentration of eFluor670 reversed, that is, *Itgb7*$^{+/+}$*Foxp3*^{GFP} (WT) or *Itgb7*$^{-/-}$*Foxp3*^{GFP} (*Itgb7*$^{-/-}$) mice were labeled with 10 μmol/L or 1 μmol/L of eFluor670, respectively.

Real-Time Quantitative PCR Analyses

Total RNA was isolated from colon using a tissue homogenizer (JXFSTPRP-24; ThunderSci, Shanghai, China) and TRIzol reagent according to the manufacturer's protocol (Thermo Fisher Scientific, Waltham, MA). For gene expression analysis, single-stranded complementary DNA was produced from 10 μg colonic total RNA using SuperScript III First-Strand synthesis and oligo-dT (deoxythymine) primers according to the manufacturer's protocol (Thermo Fisher Scientific). The kappa SybrFast quantitative PCR kit (Kapa Biosystems, Wilmington, MA) and thermal cycler (CFX96 Real-Time System; Bio-Rad Laboratories, Berkeley, CA) were used to determine the relative levels of the genes analyzed (primer sequences are shown in Table 3) according to the manufacturer's protocol. The 2–delta delta CT ($^{-\Delta\Delta CT}$) method was used for analysis, and data were normalized to glyceraldehyde-3-phosphate dehydrogenase. Control values (WT mice or *Rag1*$^{-/-}$ mice injected with phosphate-buffered saline) were set to 1 for comparisons.

Statistical Analysis

Statistical analysis was performed using PRISM software (version 6.00, GraphPad Software, San Diego, CA), and all data sets were checked for Gaussian normality distribution. Data analysis was performed using a 2-tailed *t* test, 1-way or 2-way analysis of variance, followed by the Bonferroni

Table 3. Primers for Quantitative PCR

IL1β	F	AGTGTGGATCCCAAGCAATAC
	R	CTCCACTTTGCTCTTGACTTCT
TNF-α	F	AGTGACAAGCCTGTAGCCC
	R	GAGGTTGACTTTCTCCTGGTAT
IL6	F	CTGCAAGAGACTTCCATCCAGTT
	R	GAAGTAGGGAAGGCCGTGG
IFNγ	F	CTCTTCCTCATGGCTGTTTCT
	R	TTCTTCCACATCTATGCCACTT
IL17	F	TCTCCACCGCAATGAAGACC
	R	CACACCCACCAGCATCTTCT
GAPDH	F	CCAGGTTGTCTCCTGCGACTT
	R	CCTGTTGCTGTAGCCGTATTCA

F, forward; GAPDH, glyceraldehyde-3-phosphate dehydrogenase; IFN, interferon; R, reverse; TNF, tumor necrosis factor.

posttest as indicated in the figure legends. The resulting P values are indicated as follows: *, $.01 < P < .05$; **, $.001 < P < .01$; ***, $P < .001$. Plotted data are the means ± SEM of at least 3 independent experiments.

References

1. de Souza HS, Fiocchi C. Immunopathogenesis of IBD: current state of the art. Nat Rev Gastroenterol Hepatol 2016;13:13–27.
2. Macdonald TT, Monteleone G. Immunity, inflammation, and allergy in the gut. Science 2005;307:1920–1925.
3. Khor B, Gardet A, Xavier RJ. Genetics and pathogenesis of inflammatory bowel disease. Nature 2011; 474:307–317.
4. Thomas S, Baumgart DC. Targeting leukocyte migration and adhesion in Crohn's disease and ulcerative colitis. Inflammopharmacology 2012;20:1–18.
5. Eksteen B, Liaskou E, Adams DH. Lymphocyte homing and its role in the pathogenesis of IBD. Inflamm Bowel Dis 2008;14:1298–1312.
6. Adams DH, Eksteen B. Aberrant homing of mucosal T cells and extra-intestinal manifestations of inflammatory bowel disease. Nat Rev Immunol 2006;6:244–251.
7. Ley K, Laudanna C, Cybulsky MI, Nourshargh S. Getting to the site of inflammation: the leukocyte adhesion cascade updated. Nat Rev Immunol 2007;7:678–689.
8. Fantini MC, Monteleone G. Update on the therapeutic efficacy of Tregs in IBD: thumbs up or thumbs down? Inflamm Bowel Dis 2017;23:1682–1688.
9. Danese S. New therapies for inflammatory bowel disease: from the bench to the bedside. Gut 2012; 61:918–932.
10. Strober W, Fuss I, Mannon P. The fundamental basis of inflammatory bowel disease. J Clin Invest 2007; 117:514–521.
11. Weninger W, Biro M, Jain R. Leukocyte migration in the interstitial space of non-lymphoid organs. Nat Rev Immunol 2014;14:232–246.
12. Nourshargh S, Hordijk PL, Sixt M. Breaching multiple barriers: leukocyte motility through venular walls and the interstitium. Nat Rev Mol Cell Biol 2010;11:366–378.
13. Sun H, Liu J, Zheng Y, Pan Y, Zhang K, Chen J. Distinct chemokine signaling regulates integrin ligand specificity to dictate tissue-specific lymphocyte homing. Dev Cell 2014;30:61–70.
14. Neurath MF. Current and emerging therapeutic targets for IBD. Nat Rev Gastroenterol Hepatol 2017; 14:269–278.
15. Feagan BG, Rutgeerts P, Sands BE, Hanauer S, Colombel JF, Sandborn WJ, Van Assche G, Axler J, Kim HJ, Danese S, Fox I, Milch C, Sankoh S, Wyant T, Xu J, Parikh A. Vedolizumab as induction and maintenance therapy for ulcerative colitis. N Engl J Med 2013; 369:699–710.
16. Sandborn WJ, Feagan BG, Rutgeerts P, Hanauer S, Colombel JF, Sands BE, Lukas M, Fedorak RN, Lee S, Bressler B, Fox I, Rosario M, Sankoh S, Xu J, Stephens K, Milch C, Parikh A. Vedolizumab as induction and maintenance therapy for Crohn's disease. N Engl J Med 2013;369:711–721.
17. Barre A, Colombel JF, Ungaro R. Review article: predictors of response to vedolizumab and ustekinumab in inflammatory bowel disease. Aliment Pharmacol Ther 2018;47:896–905.
18. Peyrin-Biroulet L, Danese S, Argollo M, Pouillon L, Peppas S, Gonzalez-Lorenzo M, Lytras T, Bonovas S. Loss of response to vedolizumab and ability of dose intensification to restore response in patients with Crohn's disease or ulcerative colitis: a systematic review and meta-analysis. Clin Gastroenterol Hepatol 2019; 17:838–846 e2.
19. Vermeire S, O'Byrne S, Keir M, Williams M, Lu TT, Mansfield JC, Lamb CA, Feagan BG, Panes J, Salas A, Baumgart DC, Schreiber S, Dotan I, Sandborn WJ, Tew GW, Luca D, Tang MT, Diehl L, Eastham-Anderson J, De Hertogh G, Perrier C, Egen JG, Kirby JA, van Assche G, Rutgeerts P. Etrolizumab as induction therapy for ulcerative colitis: a randomised, controlled, phase 2 trial. Lancet 2014;384:309–318.
20. Maul J, Loddenkemper C, Mundt P, Berg E, Giese T, Stallmach A, Zeitz M, Duchmann R. Peripheral and intestinal regulatory CD4+ CD25(high) T cells in inflammatory bowel disease. Gastroenterology 2005; 128:1868–1878.
21. Li Z, Arijs I, De Hertogh G, Vermeire S, Noman M, Bullens D, Coorevits L, Sagaert X, Schuit F, Rutgeerts P, Ceuppens JL, Van Assche G. Reciprocal changes of Foxp3 expression in blood and intestinal mucosa in IBD patients responding to infliximab. Inflamm Bowel Dis 2010;16:1299–1310.
22. Neurath MF. Cytokines in inflammatory bowel disease. Nat Rev Immunol 2014;14:329–342.
23. Wong E, Cohen T, Romi E, Levin M, Peleg Y, Arad U, Yaron A, Milla ME, Sagi I. Harnessing the natural inhibitory domain to control TNFalpha converting enzyme (TACE) activity in vivo. Sci Rep 2015;6:35598.
24. Desreumaux P, Foussat A, Allez M, Beaugerie L, Hebuterne X, Bouhnik Y, Nachury M, Brun V, Bastian H, Belmonte N, Ticchioni M, Duchange A, Morel-Mandrino P, Neveu V, Clerget-Chossat N, Forte M, Colombel JF. Safety and efficacy of antigen-specific regulatory T-cell therapy for patients with refractory Crohn's disease. Gastroenterology 2012; 143:1207–1217, e1–2.
25. Maynard CL, Harrington LE, Janowski KM, Oliver JR, Zindl CL, Rudensky AY, Weaver CT. Regulatory T cells expressing interleukin 10 develop from Foxp3+ and Foxp3- precursor cells in the absence of interleukin 10. Nat Immunol 2007;8:931–941.
26. Rubtsov YP, Rasmussen JP, Chi EY, Fontenot J, Castelli L, Ye X, Treuting P, Siewe L, Roers A, Henderson WR Jr, Muller W, Rudensky AY. Regulatory T cell-derived interleukin-10 limits inflammation at environmental interfaces. Immunity 2008;28:546–558.
27. Kuhn R, Lohler J, Rennick D, Rajewsky K, Muller W. Interleukin-10-deficient mice develop chronic enterocolitis. Cell 1993;75:263–274.

28. Zhang J, Fu S, Sun S, Li Z, Guo B. Inflammasome activation has an important role in the development of spontaneous colitis. Mucosal Immunol 2014; 7:1139–1150.
29. Fischer A, Zundler S, Atreya R, Rath T, Voskens C, Hirschmann S, Lopez-Posadas R, Watson A, Becker C, Schuler G, Neufert C, Atreya I, Neurath MF. Differential effects of alpha4beta7 and GPR15 on homing of effector and regulatory T cells from patients with UC to the inflamed gut in vivo. Gut 2015;65:1642–1664.
30. Denning TL, Kim G, Kronenberg M. Cutting edge: CD4+CD25+ regulatory T cells impaired for intestinal homing can prevent colitis. J Immunol 2005; 174:7487–7491.
31. Zhang HL, Zheng YJ, Pan YD, Xie C, Sun H, Zhang YH, Yuan MY, Song BL, Chen JF. Regulatory T-cell depletion in the gut caused by integrin beta deficiency exacerbates DSS colitis by evoking aberrant innate immunity. Mucosal Immunol 2016;9:391–400.
32. Holgersen K, Kvist PH, Markholst H, Hansen AK, Holm TL. Characterisation of enterocolitis in the piroxicam-accelerated interleukin-10 knock out mouse–a model mimicking inflammatory bowel disease. J Crohns Colitis 2014;8:147–160.
33. Su W, Wynne J, Pinheiro EM, Strazza M, Mor A, Montenont E, Berger J, Paul DS, Bergmeier W, Gertler FB, Philips MR. Rap1 and its effector RIAM are required for lymphocyte trafficking. Blood 2015; 126:2695–2703.
34. Song-Zhao GX, Maloy KJ. Experimental mouse models of T cell-dependent inflammatory bowel disease. Methods Mol Biol 2014;1193:199–211.
35. Chassaing B, Aitken JD, Malleshappa M, Vijay-Kumar M. Dextran sulfate sodium (DSS)-induced colitis in mice. Curr Protoc Immunol 2014;104:Unit 15 25.
36. Hall LJ, Faivre E, Quinlan A, Shanahan F, Nally K, Melgar S. Induction and activation of adaptive immune populations during acute and chronic phases of a murine model of experimental colitis. Dig Dis Sci 2011; 56:79–89.
37. Rivera-Nieves J, Olson T, Bamias G, Bruce A, Solga M, Knight RF, Hoang S, Cominelli F, Ley K. L-selectin, alpha 4 beta 1, and alpha 4 beta 7 integrins participate in CD4+ T cell recruitment to chronically inflamed small intestine. J Immunol 2005;174:2343–2352.
38. Kato S, Hokari R, Matsuzaki K, Iwai A, Kawaguchi A, Nagao S, Miyahara T, Itoh K, Ishii H, Miura S. Amelioration of murine experimental colitis by inhibition of mucosal addressin cell adhesion molecule-1. J Pharmacol Exp Ther 2000;295:183–189.
39. Teramoto K, Miura S, Tsuzuki Y, Hokari R, Watanabe C, Inamura T, Ogawa T, Hosoe N, Nagata H, Ishii H, Hibi T. Increased lymphocyte trafficking to colonic microvessels is dependent on MAdCAM-1 and C-C chemokine mLARC/CCL20 in DSS-induced mice colitis. Clin Exp Immunol 2005;139:421–428.
40. Agace WW. Tissue-tropic effector T cells: generation and targeting opportunities. Nat Rev Immunol 2006; 6:682–692.
41. Neurath MF. New targets for mucosal healing and therapy in inflammatory bowel diseases. Mucosal Immunol 2014;7:6–19.
42. Coskun M, Vermeire S, Nielsen OH. Novel targeted therapies for inflammatory bowel disease. Trends Pharmacol Sci 2017;38:127–142.
43. Luck H, Tsai S, Chung J, Clemente-Casares X, Ghazarian M, Revelo XS, Lei H, Luk CT, Shi SY, Surendra A, Copeland JK, Ahn J, Prescott D, Rasmussen BA, Chng MH, Engleman EG, Girardin SE, Lam TK, Croitoru K, Dunn S, Philpott DJ, Guttman DS, Woo M, Winer S, Winer DA. Regulation of obesity-related insulin resistance with gut anti-inflammatory agents. Cell Metab 2015;21:527–542.
44. Schippers A, Muschaweck M, Clahsen T, Tautorat S, Grieb L, Tenbrock K, Gassler N, Wagner N. beta7-Integrin exacerbates experimental DSS-induced colitis in mice by directing inflammatory monocytes into the colon. Mucosal Immunol 2016;9:527–538.
45. Gorfu G, Rivera-Nieves J, Hoang S, Abbott DW, Arbenz-Smith K, Azar DW, Pizarro TT, Cominelli F, McDuffie M, Ley K. Beta7 integrin deficiency suppresses B cell homing and attenuates chronic ileitis in SAMP1/YitFc mice. J Immunol 2010;185:5561–5568.
46. Paul G, Khare V, Gasche C. Inflamed gut mucosa: downstream of interleukin-10. Eur J Clin Invest 2012; 42:95–109.
47. Xu M, Pokrovskii M, Ding Y, Yi R, Au C, Harrison OJ, Galan C, Belkaid Y, Bonneau R, Littman DR. c-MAF-dependent regulatory T cells mediate immunological tolerance to a gut pathobiont. Nature 2018; 554:373–377.
48. Zaki MH, Boyd KL, Vogel P, Kastan MB, Lamkanfi M, Kanneganti TD. The NLRP3 inflammasome protects against loss of epithelial integrity and mortality during experimental colitis. Immunity 2010;32:379–391.
49. Sun H, Wu Y, Qi J, Pan Y, Ge G, Chen J. The CC' and DE loops in Ig domains 1 and 2 of MAdCAM-1 play different roles in MAdCAM-1 binding to low- and high-affinity integrin alpha4beta7. J Biol Chem 2011; 286:12086–12092.
50. Fontenot JD, Dooley JL, Farr AG, Rudensky AY. Developmental regulation of Foxp3 expression during ontogeny. J Exp Med 2005;202:901–906.
51. Berlin C, Bargatze RF, Campbell JJ, von Andrian UH, Szabo MC, Hasslen SR, Nelson RD, Berg EL, Erlandsen SL, Butcher EC. alpha 4 integrins mediate lymphocyte attachment and rolling under physiologic flow. Cell 1995;80:413–422.
52. Erben U, Loddenkemper C, Doerfel K, Spieckermann S, Haller D, Heimesaat MM, Zeitz M, Siegmund B, Kuhl AA. A guide to histomorphological evaluation of intestinal inflammation in mouse models. Int J Clin Exp Pathol 2014;7:4557–4576.
53. Haeryfar SM, Hickman HD, Irvine KR, Tscharke DC, Bennink JR, Yewdell JW. Terminal deoxynucleotidyl transferase establishes and broadens antiviral CD8+ T cell immunodominance hierarchies. J Immunol 2008; 181:649–659.

Received July 5, 2019. Accepted October 30, 2019.

Correspondence
Address correspondence to: Mark H. Ginsberg, MD, Department of Medicine, University of California San Diego, 9500 Gilman Drive, MC 0726, La Jolla, California 92096. e-mail: mhginsberg@ucsd.edu.

Author contributions
Hao Sun and Mark H. Ginsberg conceived the project and designed the experiments; Hao Sun and Wun Kuk performed the experiments; Hao Sun analyzed the data; Jesús Rivera-Nieves, Miguel Alejandro Lopez-Ramirez, and Lars Eckmann contributed expert advice to the design of the experiments; and Hao Sun and Mark H. Ginsberg wrote the manuscript with contributions from all authors.

Conflicts of interest
The authors disclose no conflicts.

Funding
This work was supported by grants HL 139947 (M.H.G.), HL133530 (M.A.L.R.) and DK120515 (L.E) from the National Institutes of Health, United States; the grant 17POST33660181 (H.S.) from the American Heart Association, United States.